

Journal of Advanced Pharmacy Research



Section E: Microbiology & Immunology

Synthesis, *In Silico* and *In Vitro* Antimicrobial Evaluation of Cyanoketene *S,N*-Acetals and their Pyrazoles Against *Staphylococcus aureus* DNA Gyrase Enzyme

Shima Mahmoud Ali*¹, Ahmed H.I. Faraag², Hossam R. Elgiushy³, Taghrid S. El-Mahdy^{1,4}, Ahmed A. Askar⁴, Ashraf S. Hassan⁵, Khaled A. M. Abouzid^{6,7}, Sherif F. Hammad*^{3,9}

¹Department of Microbiology and Immunology, Faculty of Pharmacy, Helwan University, Egypt. ² Department of Botany and Microbiology, Faculty of Science, Helwan University, Cairo, Egypt. ³ Pharmaceutical Chemistry Department, Faculty of Pharmacy, Helwan University, Cairo, Egypt. ⁴Department of Microbiology and Immunology, Faculty of Pharmacy, Ahran Canadian University, Giza, Egypt. ⁵Botany and Microbiology Department, Faculty of Science (Boys), Al-Azhar University, Cairo, Egypt. ⁶Organometallic and Organometalloid Chemistry Department, National Research Centre, Dokki, Cairo 12622, Egypt. ⁷Department of Pharmaceutical Chemistry, Faculty of Pharmacy, Ain Shams University, Cairo, Egypt. ⁸Department of organic and medicinal chemistry, Faculty of Pharmacy, Sadat City University, Sadat City, Egypt. ⁹Basic and Applied Sciences Institute, Egypt-Japan University of Science and Technology (E-JUST), New Borg El-Arab City, 21934 Alexandria, Egypt.

*Corresponding authors: Shima Mahmoud Ali, Department of Microbiology and Immunology, Faculty of Pharmacy, Helwan University, Cairo, Egypt. Tel. (+2)01012436536 Email address: Shaima.mn@gmail.com

Sherif F. Hammad, Pharmaceutical Chemistry Department, Faculty of Pharmacy, Helwan University, Cairo, Egypt. Tel. (+2)01013747382 Email address: Sherifhammad2010@hotmail.com

Submitted on: 13-05-2021; Revised on: 13-06-2021; Accepted on: 16-06-2021

To cite this article: Ali, S. M.; Farrag, A. H. I.; Elgiushy, H. R.; El-Mahdy, T. S.; Askar, A. A.; Hassan, A.S; Abouzid, K. A. M.; Hammad, S. F. Synthesis, *In Silico* and *In Vitro* Antimicrobial Evaluation of Cyanoketene *S,N*-Acetals and their Pyrazoles Against *Staphylococcus aureus* DNA Gyrase Enzyme. *J. Adv. Pharm. Res.* **2021**, 5 (3), 341-361. DOI: [10.21608/aprh.2021.76173.1130](https://doi.org/10.21608/aprh.2021.76173.1130)

ABSTRACT

Objectives: The continuous reporting of bacterial resistance to antibiotics is an ongoing challenge that can be life-threatening. Actions to develop new chemicals to overcome the bacterial resistance has gained a significant importance. **Methods:** A series of ketene *S,N*-acetals **4a-k** and their pyrazoles **6a-k** were synthesized and their structures were established by spectral data. Membrane permeability predictions and *in vitro* antimicrobial activity against multi-drug resistant (MDR) Gram-positive bacteria and other microorganisms was determined. The binding affinity with DNA gyrase was assessed using *in silico* studies in comparison to ciprofloxacin then the gyrase inhibition assay was conducted to detect the mode of action. **Results:** All the synthesized compounds have a good affinity to pass through the phospholipid membrane of *Staphylococcus aureus* (*S. aureus*). Compound **6g** exhibited the most potent antibacterial activity with MIC values ranged between 16 and 32 µg/mL. The compound also showed a higher binding affinity than ciprofloxacin with DNA gyrase in the *in silico* studies and this effect was clearly shown by a very good IC₅₀ value of the gyrase inhibition assay. **Conclusions:** According to our data, compound **6g** is a possible candidate to act against MDR bacteria and its main mode of action is through inhibition of the gyrase enzyme, further modifications are still required to enhance its activity.

Keywords: Acrylamide; 5-Aminopyrazole; DNA gyrase; Multi-drug resistance.

INTRODUCTION

The use of antibiotics has a profound impact on human life. Unfortunately, more pathogenic strains have become resistant to antibiotics and chemotherapeutic agents. For example, methicillin-resistant *Staphylococcus aureus* (MRSA) is resistant to penicillins (such as methicillin). In order to develop resistance, bacteria can acquire drug resistance plasmids to one or more drugs. Bacteria can also increase the expression of genes that code for multidrug efflux pumps¹. MRSA strains contain penicillin-binding protein 2a (PBP-2a) mediated through the *mecA* gene, whose expression is induced by methicillin and other β -lactams. This protein is responsible for MRSA's resistance to β -lactam antibiotics².

Another widespread resistance is through DNA gyrase and topoisomerase IV inhibitors³. DNA gyrase is an enzyme that belongs to the class of topoisomerases, which typically relieve the problem of DNA winding by participating in the overwinding or underwinding of DNA. DNA gyrase typically removes supercoils and introduces negative supercoils into DNA⁴. Although gyrase generally requires ATP hydrolysis, it can relax negatively supercoiled DNA in an ATP-independent manner⁵. Fluoroquinolones, such as ciprofloxacin, are known to inhibit DNA gyrase⁴.

Medicinal chemists are always needed to develop new chemical entities to defend humanity against life-threatening infections⁶. Cyanoketene *S,N*-Acetals bear acrylamide moiety. Acrylamide is a chemical with a diverse range of biological activities, including antibacterial and antifungal activities⁷. Elgiushy *et al.* reported two potent acrylamide derivatives that exhibited antimicrobial activities⁸. Avalos *et al.* also reported the synthesis of set of unsaturated amides with anti-mycobacterial activity⁹. Other FDA-approved drugs which incorporate the acrylamide moiety in their structures include the antibiotics anthramycin and rifampicin. The pyrazole heterocyclic moiety also exhibits a good range of biological activities: antimalarial activities¹⁰, anti-HIV activities¹¹, anti-HCV activities¹² and anti-influenza H1N1 activities¹³. Some pyrazole derivatives also showed good activity against *S. aureus*¹⁴. Poly-substituted and condensed pyrazolo pyranopyrimidine and pyrazolo pyranotriazine exhibited potent antifungal and antibacterial activities¹⁵. Findings from a previous study highlighted the antimicrobial activities of a group of newly synthesized pyrazole derivatives¹⁶. Another study showed that pyrazole displayed higher antibacterial activity than other chemicals with heterocyclic rings such as hydrazide, triazine, isoxazole, and pyrimidine derivatives¹⁷. Ahn *et al.*, reported a compound with antimicrobial activity against multi-drug resistant (MDR) bacteria, such as MRSA, MDR

Pseudomonas aeruginosa, and vancomycin-resistant *Enterococcus faecium* strains¹⁸.

Building upon all the previously described and in continuation of our target¹⁹⁻²⁸, we have herein synthesized a series of acrylamides (ketene *S,N*-acetals) and their 5-aminopyrazoles. In this study we focused on testing the antimicrobial activity of acrylamide and pyrazole moieties in a trial to find a solution to the very challenging increasing resistance of MDR Gram-positive bacteria.

MATERIAL AND METHODS

Chemistry

All melting points were measured on a Gallenkamp melting point apparatus and are uncorrected. The IR spectra were recorded (KBr disk) on a Perkin Elmer 1650 FT-IR instrument. ¹H NMR (400 MHz) and ¹³C NMR (100 MHz) spectra were recorded on a Varian spectrometer using DMSO-*d*₆ as solvent and TMS as an internal standard. Chemical shifts are reported in ppm. Mass spectra were recorded on a Varian MAT 112 spectrometer at 70 eV. Elemental analyses were performed at the Microanalytical Center, Cairo University, Egypt.

Progress of the reactions was monitored by thin-layer chromatography (TLC) using aluminium sheets coated with silica gel F₂₅₄ (Merck). All evaporations were carried out under reduced pressure at 40° C. Reagents and solvents used in the synthesis were purchased from Sigma-Aldrich. Compounds **1a-e** were prepared according to the reported procedure²⁹.

General procedure for the synthesis of 2-Cyano-3-(arylamino)-3-(methylthio)-N-(substituted) acrylamides **4a-k**

A mixture of cyanoacetamides **1a-e** (0.01 mol) and isothiocyanates (0.01 mol) was heated by hot plate for 5-10 min in ethanol (25 ml) containing potassium hydroxide (0.01 mol). After cooling, methyl iodide (0.01 mol) was added. The reaction mixture was stirred at room temperature for 1 hour and then poured onto ice water. The precipitated product was filtered and recrystallized from ethanol.

2-Cyano-3-(methylthio)-3-(phenylamino) acrylamide (**4a**). White crystals; yield 76%; m.p. 162 °C³⁰.

2-Cyano-3-(methylthio)-N-phenyl-3-(phenylamino) acrylamide (**4b**). White crystals; yield 85%; m.p. 124 °C³¹.

2-Cyano-3-(methylthio)-N-(4-methylphenyl)-3-(phenylamino) acrylamide (**4c**). White crystals; yield 82%; m.p. 120 °C³¹.

2-Cyano-3-(4-methoxyphenylamino)-3-(methylthio) acrylamide (**4d**). White crystals; yield 79%; m.p. 160 °C³².

2-Cyano-3-[(4-methoxyphenyl) amino]-3-(methylthio)-N-phenylacrylamide (**4e**). Light yellow prisms; yield 71%; m.p. 103 °C³³.

2-Cyano-3-[(4-methoxyphenyl)amino]-N-(4-methylphenyl)-3-(methylthio)acrylamide (**4f**). Colorless prisms; yield 75%; m.p. 177 °C³³.

N-(4-Chlorophenyl)-2-cyano-3-[(4-methoxyphenyl) amino]-3-(methylthio)acrylamide (**4g**). White crystals; yield 70%; m.p. 156-157 °C³³.

2-Cyano-3-(2,4-dimethoxyphenylamino)-3-(methylthio)acrylamide (**4h**). Yellow crystals; yield 85%; m.p. 155-157 °C; IR (KBr) $\nu_{\max}/\text{cm}^{-1}$ 3381, 3198, 3007 (NH₂, NH), 2194 (C≡N), 1654 (C=O). ¹H NMR (400 MHz, DMSO-*d*₆): δ 2.11 (s, 3H, SCH₃), 3.66, 3.67 (2s, 6H, 2OCH₃), 6.47, 6.49 (dd, 1H, Ar-H, *J* = 2.6 & 8.5 Hz), 6.50 (d, 1H, Ar-H, *J* = 2.4 Hz), 7.24 (d, 1H, Ar-H, *J* = 8.4 Hz), 7.28 (s, 2H, NH₂), 11.85 (s, 1H, NH). ¹³C NMR (100 MHz, DMSO-*d*₆): δ 16.53 (-SCH₃), 55.55 & 55.95 (-2OCH₃), 76.71 (C₂, acrylamide), 99.06, 104.79 (2C, Ar), 119.05 (C≡N), 119.55, 126.79, 154.19, 159.28 (4C, Ar), 168.63 (C=O), 168.80 (C₃, acrylamide). MS (m/z, %): 292.89 (M⁺, 22.88), 76.96 (100, Bp). Anal. Calcd. (%) for C₁₃H₁₅N₃O₃S (293.34): C, 53.23; H, 5.15; N, 14.32. Found: C, 53.15; H, 5.20; N, 14.40% (see S1).

2-Cyano-3-(2,4-dimethoxyphenylamino)-3-(methylthio)-N-phenylacrylamide (**4i**). Yellow crystals; yield 79%; m.p. 132-134 °C; IR (KBr) $\nu_{\max}/\text{cm}^{-1}$ 3381, 3198, 3007 (NH₂, NH), 2194 (C≡N), 1654 (C=O). ¹H NMR (400 MHz, DMSO-*d*₆): δ 2.25 (s, 3H, SCH₃), 3.78, 3.82 (2s, 6H, 2OCH₃), 6.55, 6.57 (dd, 1H, Ar-H, *J* = 2.5 & 8.7 Hz), 6.68 (d, 1H, Ar-H, *J* = 2.5 Hz), 7.07 (t, 1H, Ar-H), 7.29 (t, 2H, Ar-H), 7.30 (d, 1H, Ar-H, *J* = 8.2 Hz), 7.55 (d, 2H, Ar-H, *J* = 7.8 Hz), 9.44 (s, 1H, NH), 11.80 (s, 1H, NH). ¹³C NMR (100 MHz, DMSO-*d*₆): δ 16.65 (-SCH₃), 55.50 & 55.96 (-2OCH₃), 77.61 (C₂, acrylamide), 99.09, 104.84 (2C, Ar), 119.56 (C≡N), 121.33, 123.83, 126.60, 128.48, 138.22, 154.04, 159.37 (10C, Ar), 165.44 (C=O), 168.98 (C₃, acrylamide). MS (m/z, %): 369.05 (M⁺, 8.09), 40.12 (100, Bp). Anal. Calcd. (%) for C₁₉H₁₉N₃O₃S (369.44): C, 61.77; H, 5.18; N, 11.37. Found: C, 61.80; H, 5.15; N, 11.40% (see S2).

2-Cyano-3-(2,4-dimethoxyphenylamino)-3-(methylthio)-N-(4-methylphenyl)acrylamide (**4j**). Yellow crystals; yield 90%; m.p. 167 °C; IR (KBr) $\nu_{\max}/\text{cm}^{-1}$ 3381, 3198, 3007 (NH₂, NH), 2194 (C≡N), 1654 (C=O). ¹H NMR (400 MHz, DMSO-*d*₆): δ 2.24 (s, 3H, CH₃), 2.25 (s, 3H, SCH₃), 3.78, 3.82 (2s, 6H, 2OCH₃), 6.55, 6.57 (dd, 1H, Ar-H, *J* = 2.6 & 8.7 Hz), 6.68 (d, 1H, Ar-H, *J* = 2.6 Hz), 7.09 (d, 2H, Ar-H, *J* = 8.3 Hz), 7.30 (d, 1H, Ar-H, *J* = 8.7 Hz), 7.42 (d, 2H, Ar-H, *J* = 8.4 Hz), 9.34 (s, 1H, NH), 11.82 (s, 1H, NH). ¹³C NMR (100 MHz, DMSO-*d*₆): δ 16.62 (-SCH₃), 20.46 (-CH₃), 55.48 & 55.94 (-2OCH₃), 77.65 (C₂, acrylamide), 99.07, 104.81 (2C, Ar), 118.69 (C≡N), 119.57, 121.37, 126.56, 128.86, 132.86, 135.61,

154.03, 159.32 (10C, Ar), 165.26 (C=O), 168.74 (C₃, acrylamide). MS (m/z, %): 383.35 (M⁺, 17.39), 51.93 (100, Bp). Anal. Calcd. (%) for C₂₀H₂₁N₃O₃S (383.46): C, 62.64; H, 5.52; N, 10.96. Found: C, 62.60; H, 5.55; N, 11.00 % (see S3)

2-Cyano-N-(2,4-dimethoxyphenyl)-3-(2,4-dimethoxyphenylamino)-3-(methylthio)acrylamide (**4k**). Yellow crystals; yield 89%; m.p. 174-176 °C; IR (KBr) $\nu_{\max}/\text{cm}^{-1}$ 3381, 3198, 3007 (NH₂, NH), 2194 (C≡N), 1654 (C=O). ¹H NMR (400 MHz, DMSO-*d*₆): δ 2.24 (s, 3H, SCH₃), 3.75, 3.78, 3.82, 3.84 (4s, 12H, 4OCH₃), 6.49, 6.51 (dd, 1H, Ar-H, *J* = 2.6 & 8.8 Hz), 6.56, 6.58 (dd, 1H, Ar-H, *J* = 2.6 & 8.7 Hz), 6.66 (d, 1H, Ar-H, *J* = 2.6 Hz), 6.68 (d, 1H, Ar-H, *J* = 2.5 Hz), 7.31 (d, 1H, Ar-H, *J* = 8.7 Hz), 7.77 (d, 1H, Ar-H, *J* = 8.8 Hz), 8.33 (s, 1H, NH), 11.90 (s, 1H, NH). ¹³C NMR (100 MHz, DMSO-*d*₆): δ 16.70 (-SCH₃), 55.37, 55.53, 55.97 & 56.11 (-4OCH₃), 77.31 (C₂, acrylamide), 98.81, 99.05, 104.27, 104.83 (4C, Ar), 118.96 (C≡N), 119.33, 119.79, 122.18, 126.73, 150.79, 154.09, 156.87, 159.43 (8C, Ar), 164.46 (C=O), 168.38 (C₃, acrylamide). MS (m/z, %): 429.25 (M⁺, 24.05), 102.98 (100, Bp). Anal. Calcd. (%) for C₂₁H₂₃N₃O₅S (429.49): C, 58.73; H, 5.40; N, 9.78. Found: C, 58.70; H, 5.45; N, 9.80 % (see S4)

General procedure for the synthesis of 5-Amino-N-(substituted)-3-[arylamino]-1H-pyrazole-4-carboxamides 6a-k

A mixture of compounds **4a-k** (0.01 mol), hydrazine hydrate (**5**) (0.01 mol) and few drops of triethylamine in ethanol (30 ml) was refluxed for 4 h and then the solvent evaporated under reduced pressure. The resulting solid product was collected by filtration and recrystallized from ethanol.

5-Amino-3-(phenylamino)-1H-pyrazole-4-carboxamide (**6a**). White crystals; yield 76%; m.p. 180 °C³⁰.

5-Amino-N-phenyl-3-(phenylamino)-1H-pyrazole-4-carboxamide (**6b**). White crystals; yield 73%; m.p. 245 °C³¹.

5-Amino-3-(phenylamino)-N-(4-methylphenyl)-1H-pyrazole-4-carboxamide (**6c**). White crystals; yield 75%; m.p. 180 °C³¹.

5-Amino-3-(4-methoxyphenylamino)-1H-pyrazole-4-carboxamide (**6d**). White crystals; yield 82%; m.p. 202 °C³².

5-Amino-3-[(4-methoxyphenyl)amino]-N-phenyl-1H-pyrazole-4-carboxamide (**6e**). White crystals; yield 75%; m.p. 175 °C³³.

5-Amino-3-[(4-methoxyphenyl)amino]-N-(4-methylphenyl)-1H-pyrazole-4-carboxamide (**6f**). White crystals; yield 82%; m.p. 200-201 °C³³.

5-Amino-N-(4-chlorophenyl)-3-[(4-methoxyphenyl)amino]-1H-pyrazole-4-carboxamide (**6g**). White crystals; yield 80%; m.p. 190-191 °C³³.

5-Amino-3-(2,4-dimethoxyphenylamino)-1H-pyrazole-4-carboxamide (6h). White crystals; yield 60%; m.p. 257-259 °C; IR (KBr) $\nu_{\max}/\text{cm}^{-1}$ 3403, 3305, 3200 (NH₂, NH), 1651 (C=O). ¹H NMR (400 MHz, DMSO-*d*₆): δ 3.69, 3.81 (2s, 6H, 2OCH₃), 5.68 (s, 2H, NH₂), 6.40, 6.42 (dd, 1H, Ar-H, *J* = 2.6 & 8.8 Hz), 6.54 (d, 1H, Ar-H, *J* = 2.5 Hz), 6.56 (s, 2H, NH₂), 8.05 (d, 1H, Ar-H, *J* = 8.7 Hz), 9.18 (s, 1H, NH), 10.78 (s, 1H, NH). ¹³C NMR (100 MHz, DMSO-*d*₆): δ 55.27 & 55.73 (-2OCH₃), 85.48 (C₄, pyrazole), 98.66, 103.70, 115.51, 125.77, 146.66 (5C, Ar), 147.43 (C₅, pyrazole), 152.28 (C₃, pyrazole), 152.47 (C, Ar), 166.63 (C=O, amide). LMS (m/z, %): 277.6 (M⁺, 10), 260.81 (100, Bp). Anal. Calcd. (%) for C₁₂H₁₅N₅O₃ (277.28): C, 51.98; H, 5.45; N, 25.26. Found: C, 52.00; H, 5.40; N, 25.20% (see S5)

5-Amino-3-(2,4-dimethoxyphenylamino)-N-phenyl-1H-pyrazole-4-carboxamide (6i). White crystals; yield 55%; m.p. 127-129 °C; IR (KBr) $\nu_{\max}/\text{cm}^{-1}$ 3334, 3232 (NH₂, NH), 1641 (C=O). ¹H NMR (400 MHz, DMSO-*d*₆): δ 3.71, 3.85 (2s, 6H, 2OCH₃), 5.87 (s, 2H, NH₂), 6.45 (d, 1H, Ar-H, *J* = 7.1 Hz), 6.59 (s, 1H, Ar-H), 7.04 (s, 1H, Ar-H), 7.32 (s, 2H, Ar-H), 7.58 (d, 2H, Ar-H, *J* = 6.5 Hz), 8.04 (d, 1H, Ar-H, *J* = 1.4 Hz), 8.73 (s, 1H, NH), 8.81 (s, 1H, NH), 11.16 (s, 1H, NH). ¹³C NMR (100 MHz, DMSO-*d*₆): δ 55.30 & 55.85 (-2OCH₃), 87.30 (C₄, pyrazole), 98.75, 103.81, 115.80, 120.32, 122.91, 125.58, 128.59, 139.08, 146.86 (11C, Ar), 147.69 (C₅, pyrazole), 151.93 (C₃, pyrazole), 152.68 (C, Ar), 163.41 (C=O, amide). MS (m/z, %): 353.38 (M⁺, 13.21), 299.21 (100, Bp). Anal. Calcd. (%) for C₁₈H₁₉N₅O₃ (353.38): C, 61.18; H, 5.42; N, 19.82. Found: C, 61.20; H, 5.40; N, 19.85% (see S6)

5-Amino-3-(2,4-dimethoxyphenylamino)-N-(4-methylphenyl)-1H-pyrazole-4-carboxamide (6j). White crystals; yield 75%; m.p. 181-183 °C; IR (KBr) $\nu_{\max}/\text{cm}^{-1}$ 3365, 3326, 3290 (NH₂, NH), 1648 (C=O). ¹H NMR (400 MHz, DMSO-*d*₆): δ 2.26 (s, 3H, CH₃), 3.70, 3.83 (2s, 6H, 2OCH₃), 5.83 (s, 2H, NH₂), 6.41 & 6.44 (dd, 1H, Ar-H, *J* = 2.5 & 8.8 Hz), 6.57 (d, 1H, Ar-H, *J* = 2.5 Hz), 7.11 (d, 2H, Ar-H, *J* = 8.4 Hz), 7.44 (d, 2H, Ar-H, *J* = 8.3 Hz), 8.03 (d, 1H, Ar-H, *J* = 8.6 Hz), 8.61 (s, 1H, NH), 8.79 (s, 1H, NH), 11.10 (s, 1H, NH). ¹³C NMR (100 MHz, DMSO-*d*₆): δ 20.47 (CH₃), 55.29 & 55.83 (-2OCH₃), 87.28 (C₄, pyrazole), 98.73, 103.78, 115.74, 120.39, 125.59, 128.97, 131.83, 136.49, 146.68 (11C, Ar), 147.60 (C₅, pyrazole), 152.05 (C₃, pyrazole), 152.64 (C, Ar), 163.30 (C=O, amide). MS (m/z, %): 367.01 (M⁺, 59.09), 83.94 (100, Bp). Anal. Calcd. (%) for C₁₉H₂₁N₅O₃ (367.40): C, 62.11; H, 5.76; N, 19.06. Found: C, 62.20; H, 5.70; N, 19.00% (see S7)

5-Amino-N-(2,4-dimethoxyphenyl)-3-(2,4-dimethoxyphenylamino)-1H-pyrazole-4-carboxamide (6k). White crystals; yield 70%; m.p. 155-157 °C; IR

(KBr) $\nu_{\max}/\text{cm}^{-1}$ 3365, 3326, 3290 (NH₂, NH), 1648 (C=O). ¹H NMR (400 MHz, DMSO-*d*₆): δ 3.70, 3.74, 3.77, 3.85 (4s, 12H, 4OCH₃), 5.67 (s, 2H, NH₂), 6.42 (d, 1H, Ar-H, *J* = 7.8 Hz), 6.51 (d, 1H, Ar-H, *J* = 7.5 Hz), 6.60 (d, 2H, Ar-H), 7.88 (d, 1H, Ar-H, *J* = 7.2 Hz), 8.01 (d, 1H, Ar-H, *J* = 8.2 Hz), 8.57 (s, 1H, NH), 8.72 (s, 1H, NH), 11.23 (s, 1H, NH). ¹³C NMR (100 MHz, DMSO-*d*₆): δ 55.29, 55.31, 55.80, 55.91 (4-OCH₃), 88.60 (C₄, pyrazole), 98.77, 103.80, 104.11, 115.44, 121.37, 125.90, 147.63 (10C, Ar), 150.02 (C₅, pyrazole), 152.69 (C₃, pyrazole), 155.76, 159.54 (2C, Ar), 162.92 (C=O, amide). MS (m/z, %): 413.37 (M⁺, 5.69), 294.15 (100, Bp). Anal. Calcd. (%) for C₂₀H₂₃N₅O₅ (413.43): C, 58.10; H, 5.61; N, 16.94. Found: C, 58.10; H, 5.61; N, 16.94% (see S8)

Microbiology

Microbial strains

Clinical isolates used in this study (**Table 1 and 2**) were obtained from the Biodefense and Emerging Infections Research Resources Repository (BEI Resources) and the American Type Culture Collection (ATCC). *Escherichia coli* (*E. coli*) BW25113 and JW25113 were obtained from the Coli Genetic Stock Center (CGSC), Yale University. Bacterial strains, “except *Clostridium difficile* which was incubated anaerobically on brain heart infusion supplemented (BHIS) agar (Oxoid) at 37° C for 48 hours”, were grown aerobically overnight on tryptone soy agar (TSA, Oxoid) plates at 37° C. Whereas, *Candida albicans* was incubated aerobically overnight on yeast peptone dextrose (Oxoid) agar plate at 35° C.

Minimum inhibitory concentration (MIC) and minimum bactericidal concentration (MBC) of the synthetic compounds against some clinically-important Gram-positive and Gram-negative bacteria and *C. albicans*

The MICs of the tested compounds and control drugs (**Table 1 and 2**) against clinically-relevant bacterial and fungal strains were determined using the broth microdilution method, according to guidelines outlined by the Clinical and Laboratory Standards Institute (CLSI)³⁴. All compounds to be tested were dissolved in dimethylformamide (DMF) in a concentration of 5 mg/mL. The same concentration of DMF alone was used as a control during performance of MIC test.

Microbial solution equivalent to 0.5 McFarland standard was prepared and diluted in cation-adjusted Mueller-Hinton broth (Oxoid) (for *S. aureus*, *Staphylococcus epidermidis*, and *E. coli*) or tryptone soy broth (Oxoid) (for *Enterococcus faecalis*, *E. faecium*, *Listeria monocytogenes* and *Streptococcus pneumoniae*), to achieve a bacterial concentration of about 5 × 10⁵ colony forming unit (CFU)/mL. *C. difficile* was diluted

in BHIS broth, supplemented with yeast extract, hemin and vitamin K to achieve a bacterial concentration of about 5×10^5 CFU/mL. *C. albicans* was diluted in RPMI 1640 medium with glutamine and without bicarbonate which was buffered to pH 7.0 with 0.165 M of [3-(N-morpholino) propane sulfonic acid] (MOPS) to achieve a fungal concentration of about 1.5×10^3 CFU/mL. Compounds and control drugs were added in the first row of the 96-well plates, and serially diluted with the corresponding media containing bacteria/fungi. Plates were then, incubated aerobically at 37° C for 18-20 hours (for *S. aureus*, *S. epidermidis*, *E. faecalis*, *E. faecium*, *L. monocytogenes*, *S. pneumoniae* and *E. coli*). *C. difficile* was incubated anaerobically at 37° C for 48 hours. *C. albicans* was incubated aerobically at 37° C for 24 hours. MICs reported herein are the minimum concentrations of the compounds and control drugs that could completely inhibit the visual growth of bacteria/fungi. The MBC of compounds was tested by plating 4 μ L from wells with no growth onto fresh TSA plates. Plates were incubated at 37° C for 18-20 hours before observing the microbial growth. The MBC was recorded as the lowest concentration that reduced bacterial growth by 99.9%.

***In silico* models for predicting membrane permeability**

Computationally, membrane permeability prediction of ciprofloxacin and tested ligands were investigated using the RRCK permeability predictor in the physics-based permeability prediction module within the Schrödinger's Small-Molecule Drug Discovery Suite³⁵⁻³⁷. Energy minimization for all ligands was performed using the Macro Model of Schrödinger's software³⁸⁻⁴⁰.

Protein targets docking and scoring validation

In silico computer-based studies were used to determine antibacterial drug target prediction and the modes of action of these antimicrobials. The target proteins used in this study were: D-alanine - D-alanine ligase B (ddlB) from *E. coli*, penicillin-binding protein 1A (PBP1a) from *P. aeruginosa*, Membrane-bound lytic murein transglycosylase B (mltB) from *E. coli*, DNA-dependent RNA polymerase beta subunit (repC) from *E. coli*, Isoleucyl-tRNA synthetase (ileS) from *Thermus thermophilus*, DNA gyrase subunit B and Dihydrofolate Reductase (DHFR) from *S. aureus*, and IV topoisomerase Topo IV and Dihydropteroate synthase (DHPS) from *S. pneumoniae*. Verification and validation of the docking approach for bacterial target protein were done. Schrödinger 11.9 software was used to investigate the main ligand structure **Figure 1**, which was docked to the binding site of each protein used in this study.

Docking and structure–activity relationship (SAR)

To understand the interactions of the tested compounds at the active sites of protein receptors,

topoisomerase II DNA gyrase enzymes, docking was performed with DNA Gyrase Chain B crystallographic structure of *S. aureus* (PDB ID: 3G75)⁴¹. The crystallographic structures (PDB ID: 3G7B) were retrieved from the Protein Data Bank. The model was validated using the protein preparation wizard program from the Schrödinger suite. Water molecules and small molecules present were removed from the structure prior to docking. Docking of the intended compounds was carried out in the ATP binding site using Schrödinger Maestro 11.9 software Glide (XP) extra precision module from Schrödinger⁴². *In silico* docking and superimpose calculation of ligands and one control drug such as ciprofloxacin against DNA gyrase enzyme was performed by Maestro 11.9 software⁴³. The structural formula of the three compounds was converted to a three-dimensional format using Perkin Elmer Chem Bio Office Ultra 14.0.0.117 for docking purposes. The binding sites of target proteins were visualized using Site Map tool. The best Docking Score is obtained as the most negative value for the active ligands. All compounds were prepared using the LigPrep2.9. Glide docking parameters were set to the default hard potential function. No constraints were applied for all the docking studies. SAR analysis was performed using R-Group Analysis.

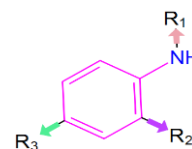
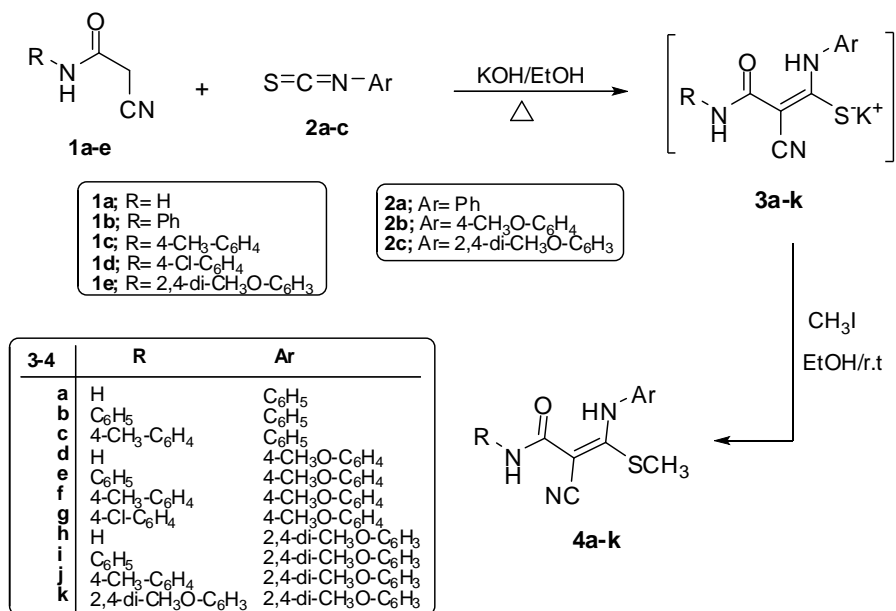


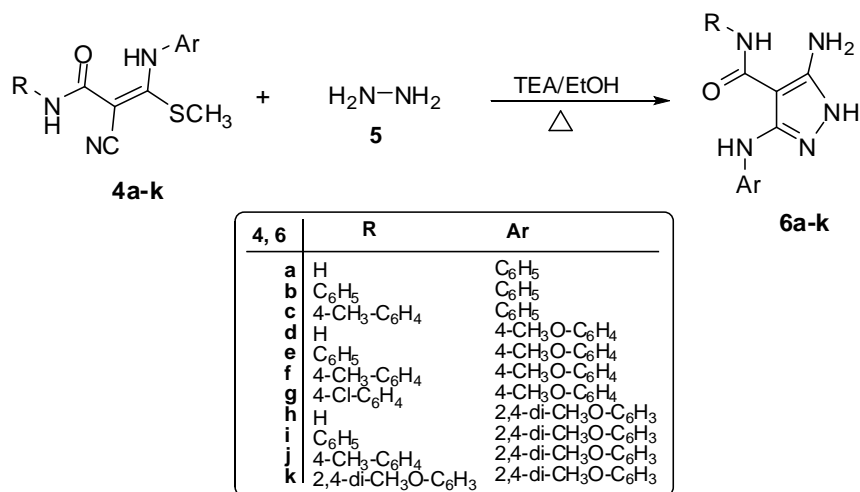
Figure 1. Main structure of the ligand with different R groups

Gyrase inhibition assay

Gyrase inhibition assay was applied on three of the test compounds selected according to their results on the above experiments. The most potent antibacterial compound (**6g**) and of the least potent compounds, we picked the one that also showed the lowest docking and QSAR values (**4a**). The third compound was the one which showed the highest docking and QSAR values of those having some antibacterial effect (**6i**). These material were used for the two following experiments (a and b): Enzyme: *S. aureus* gyrase stored at -80°C. *S. aureus* gyrase assay buffer: 40 mM HEPES. KOH (pH 7.6), 10 mM magnesium acetate, 10 mM DTT, 2 mM ATP, 500 mM potassium glutamate, 0.05 mg/ml albumin (supplied as 5X), stored at -20° C. Dilution Buffer: 50 mM Tris.HCl (pH 7.5), 1 mM DTT, 1 mM EDTA, 40% (w/v) glycerol (supplied as 1X), stored at -20 C. Plasmid: Relaxed pBR322 (supplied at 1 μ g/ μ L). Other materials not included in the kit: STEB: 40% (w/v) sucrose, 100 mM Tris-HCl pH 8, 10 mM EDTA, 0.5 mg/ml, Bromophenol Blue.



Scheme 1. Synthesis of ketene *S,N*-acetals 4a-k



Scheme 2. Synthesis of 5-aminopyrazoles 6a-k

In the two experiments below (a and B), after the enzyme addition the mixture is mixed by gentle vortexing, and incubated for 30 minutes at 37°C. The reaction was stopped by adding 30 µL of STEB and 30 µL of chloroform/isoamyl alcohol (v:v, 24:1), vortexed briefly and centrifuged for 1 minute. Twenty µL of the aqueous (upper blue) phase was loaded onto a 1% (w/v) agarose gel, run at ~75 V for approximately 2 hours or until the blue dye front has run at about 5 cm or more. The gel was stained with 1 µg/ml ethidium bromide in

water (15 min), destained (5-10 min) in water and visualized with a gel documentation system (Bio-Rad).

Determination of *S. aureus* gyrase enzyme optimal concentration

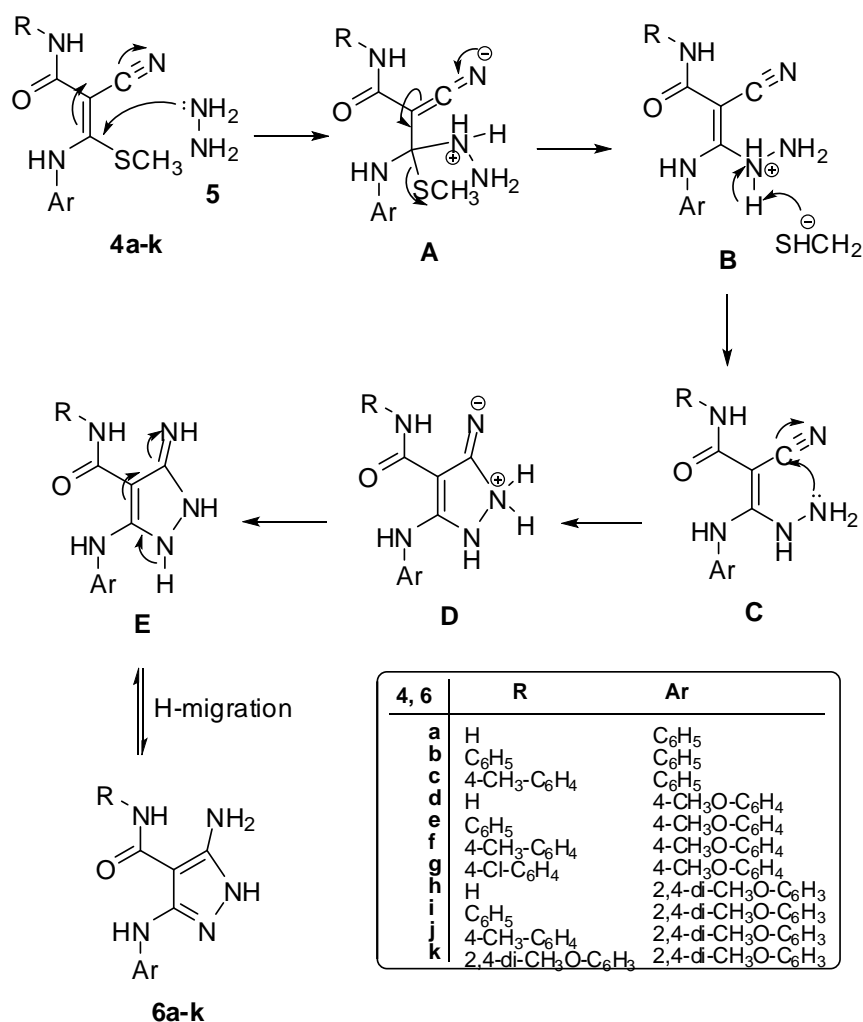
To determine the inhibitory activity of the chemical compounds on the gyrase enzyme, we first needed to determine the optimal concentration of the enzyme that gives full supercoiling. A relaxed plasmid pBR322 gets supercoiled by gyrase enzyme. The relaxed

and supercoiled forms of the plasmid can be separated by agarose gel electrophoresis which can be used to determine the enzyme activity. A gel-based supercoiling experiment with relaxed pBR322 and in the presence of 1% dimethyl sulfoxide (DMSO), was set up as follows: a mixture was prepared of 84 μL of assay Buffer (5X), 7 μL relaxed pBR322, 4.2 μL DMSO, 282.8 μL of water. Twenty-seven μL of this MIX was added to several eppendorf tubes. Serial dilutions of the enzyme were made in dilution buffer, then 3 μL was added to the reactions. It was found that approximately, 0.1 μL of the neat enzymes required to give full supercoiling (see S9), so this concentration was used for the following experiment.

Gyrase inhibition assay of the synthetic compounds

Several 24 μL mixtures of assay buffer (6 μL of 5x buffer), relaxed pBR322 (0.5 μL) and water (17.5 μL) were put in 1.5 mL-eppendorf tubes submerged in ice.

First the ciprofloxacin was tested in eight dilutions to determine the optimal set of the inhibitory concentrations to be used (see S10). Four concentrations were selected to be prepared of three tested compound and ciprofloxacin then aliquots of 3 μL of them or the solvent were added to the corresponding tubes and mixed briefly. The enzyme was diluted in dilution buffer (to the concentration determined as explained in (a), the above experiment) and added (3 μL) to all the tubes except the negative control tubes (3 μL of the dilution buffer was added instead). The supercoiled bands for each sample on the gel were photographed by gel documentation system. Then photos were scanned and the percentages of supercoiling activity or supercoiling inhibition were determined and compared to the positive control (tube containing gyrase enzyme and no inhibitor). These percentages were plotted against the inhibitor concentration (μM) and the IC_{50} was calculated from a fitted curve (see S11).



Scheme 3. Mechanism for the formation of 5-aminopyrazole 6a-k

RESULTS AND DISCUSSION

Chemistry

2-Cyanoacetamides **1a-e** reacted with isothiocyanate **2a-c** in absolute ethanol containing an equimolar of KOH to give the corresponding intermediates stable potassium 2-cyano-1-(arylamino)-3-oxo-3-(substituted-amino)prop-1-ene-1-thiolate salt **3a-k**. When the latter was alkylated with CH₃I, it generated the ketene *S,N*-acetals **4a-k** in 80–90 % yield (**Scheme 1**).

The structures of new ketene *S,N*-acetals **4a-k** were established by different spectral data. For example, the ¹H-NMR spectrum of **4j** exhibited four singlet signals at 2.24, 2.25, 3.78 and 3.82 points to –SCH₃, –CH₃ and two –OCH₃ protons, respectively. Two doublets at 7.09 and 7.42 corresponded to the aromatic protons of 4-methylphenyl (*AB* system, with *J* = 8.3 and 8.4 Hz, respectively). The *di*-substituted aromatic protons of 2,4-dimethoxyphenyl appeared as one proton as a doublet of a doublet at 6.55 and 6.57 with coupling constants *J* = 2.6 Hz and *J* = 8.7 Hz. Two protons appeared as two doublets at 6.68 (1*H*, *J* = 2.6 Hz) and 7.30 (1*H*, *J* = 8.7 Hz). Two singlet signals at 9.34 and 11.82 were assigned to two –NH protons. The ¹³C-NMR spectrum was characterized by five signals for carbons of –SCH₃, C₂ (acrylamide), C≡N, C=O and C₃ (acrylamide) at δ = 16.62, 77.65, 118.69, 165.26 and 168.74 ppm, respectively. We suggested that the structures of ketene *S,N*-acetals **4a-k** should be present in the *E* form and not in the *Z* form⁴⁴.

5-Amino-1*H*-pyrazoles **6a-k** was obtained *via* the reaction of ketene *S,N*-acetals **4a-k** with hydrazine hydrate (**5**) in refluxing ethanol in the presence of a catalytic amount of triethylamine (**Scheme 2**).

The structures of 5-amino-1*H*-pyrazoles **6a-k** were established by various spectral analyses (MS, IR, ¹H-NMR and ¹³C-NMR). The IR (ν_{max}/cm⁻¹) spectrum of 5-aminopyrazole **6h** indicated the absence of absorption bands of nitrile group and showed bands at 3305, 3200 and 1651 due to NH₂, NH and C=O functions, respectively.

Its ¹H NMR spectrum exhibited six singlet signals at δ = 3.69, 3.81, 5.68, 6.56, 9.18 and 10.78 due to OCH₃, OCH₃, NH₂, NH₂, NH and NH protons, respectively. The signal of –SCH₃ protons not appeared in its ¹H NMR spectrum. However, one proton of the aromatic ring appeared at 6.40 and 6.42 as a doublet of the doublet with coupling constants *J* = 2.6 Hz and *J* = 8.8 Hz and two doublets at 6.54 (1*H*, *J* = 2.5 Hz) and 8.05 (1*H*, *J* = 8.7 Hz) due to two protons of aromatic ring. The ¹³C-NMR exhibited characterized signals at δ = 85.48, 147.43, 152.28 and 166.63 due to C₄, C₅, C₃ (pyrazole moiety) and carbonyl function, respectively.

Additionally, we investigated and proved the structure of 5-amino-1*H*-pyrazoles **6a-k** and the possible

mechanism from previous studies by the X-ray single crystal of compound **6g** and the possible formation of 5-aminopyrazole **6a-k** is shown in **Scheme 3**^{45a and b}.

Microbiology

Susceptibility of some clinically-important Gram-positive and Gram-negative bacteria to the synthesized compounds using MIC and MBC

To evaluate the antimicrobial effect of the synthesized compounds toward several clinically relevant bacterial and fungal strains, the MICs of the compounds and control drugs were determined using the broth microdilution method. The MICs are reported in **Table 1**.

It is clear from **Table 1** that none of the tested compounds showed activity against wild type *E. coli* or *C. albicans*. On the other hand, the results show that some of our compounds showed variable antibacterial activity against the other strains tested. This finding comes in agreement with previous studies^{7,8,14-16,18} which reported that acrylamide and pyrazole derivatives have antibacterial activities. Compounds **4j** and **6c** were slightly active against MRSA USA 300, *E. coli* JW55031 (TolC mutant) and *C. difficile* ATCC BAA 1870 with MIC values ranged between 32 and 64 μg/ml. Whereas, compound **6g** exhibited the least MIC value among the tested compounds with a value of 16 μg/ml for the three strains. Based on this positive result, compound **6g** was further screened against additional clinical Gram-positive isolates of methicillin-sensitive *S. aureus*, MRSA, vancomycin-resistant *S. aureus* (VRSA), *S. epidermidis*, vancomycin-resistant *Enterococcus faecium*, vancomycin-resistant *Enterococcus faecalis* and *Streptococcus pneumonia* (**Table 2**). Additionally, we examined whether the compound was bacteriostatic (inhibits bacterial growth) or bactericidal (kills bacteria) by determining the MBC.

In agreement with the previous results of **6g** MIC values against MRSA USA300 (**Table 1**), compound **6g** exhibited a moderate to a poor activity against the tested panel of MDR strains with MIC values ranging from 16 to > 64 μg/ml. It appeared to be bactericidal to most tested strains as its MBC values were one- or two-fold higher than its corresponding MIC values.

In silico ligands membrane permeability prediction

The physical-membrane permeability based on the *in silico* model predictions can be used for drug design to predict the membrane permeability before the process of drug synthesis⁴⁶. The results are shown in **Table 3**.

The predicted relative permeabilities were based on the calculated 'Log Perm RRCK' values where a more negative value indicated that lower cell permeability⁴⁷. However, less positive value of (Membrane dG Insert) means more permeable

Table 1: MIC ($\mu\text{g/ml}$) of the synthesized compounds and control drugs using the broth microdilution method

Compounds /Control Antibiotics	Bacterial Strains				
	MRSA NRS384 (USA300)	<i>E. coli</i> JW55031 (TolC mutant)	<i>E. coli</i> BW25113 (wild-type)	<i>C. difficile</i> ATCC BAA 1870	<i>C. albicans</i> ATCC 64124
4a	> 128	128	> 128	> 128	> 128
4b	> 128	> 128	> 128	> 128	> 128
4d	> 128	> 128	> 128	> 128	> 128
4e	> 128	> 128	> 128	> 128	> 128
4f	> 128	> 128	> 128	> 128	> 128
4g	> 128	> 128	> 128	> 128	> 128
6a	> 128	> 128	> 128	> 128	> 128
6b	128	64	> 128	64	> 128
6c	64	32	> 128	32	> 128
6d	> 128	> 128	> 128	> 128	> 128
6e	> 128	64	> 128	32	> 128
6f	> 128	> 128	> 128	> 128	> 128
6g	16	16	> 128	16	> 128
4h	> 128	> 128	> 128	> 128	> 128
4i	64	> 128	> 128	> 128	> 128
4j	64	32	> 128	32	> 128
4k	> 128	> 128	> 128	> 128	> 128
6h	> 128	> 128	> 128	> 128	> 128
6i	> 128	64	> 128	64	> 128
6j	> 128	> 128	> 128	> 128	> 128
6k	> 128	64	> 128	64	> 128
Linezolid	1	8	> 64	NA	NA
Vancomycin	1	NA	NA	1	NA
Gentamycin	NA	0.5	0.5	NA	NA
Fluconazole	NA	NA	NA	NA	> 128
5-Fluorocytosine	NA	NA	NA	NA	0.25

-NA: Not applicable, the drug is not used for treating the infections caused by the tested microorganism

MRSA: Methicillin-resistant *Staphylococcus aureus*

-TolC mutant strain encodes an efflux pump

-MRSA and *Clostridium difficile* are Gram-positive bacteria; *Escherichia coli* is a Gram-negative bacterium while *Candida albicans* is a unicellular fungus

membranes. The ligands, **6k**, **6j**, **6i**, **6h**, **6g**, **6f**, **6e**, **6d**, **6c**, **6b** and **6a** showed Log Perm RRCK values close to ciprofloxacin -5.296cm/s and the membrane dG Insert value of them were 20.184, 19.062, 19.184, 20.780, 19.709, 19.002, 19.218, 20.829, 17.969, 18.260 and 20.128, respectively in comparison to 12.935 Membranes dG Insert value of ciprofloxacin. These

results indicate that the compounds have good cellular permeability to them but a bit less than ciprofloxacin. Ligands **4k**, **4j**, **4i**, **4h**, **4g**, **4f**, **4e**, **4d**, **4c**, **4b** and **4a** showed less positive values of Membrane dG Insert than reference ciprofloxacin compound and also less negative 'Log Perm RRCK' (Table 3) which means that the bacterial cell are highly permeable to those compounds

Table 2. The MIC (µg/ml) and the MBC (µg/ml) of compound 6g against a panel of pathogenic Gram-positive bacteria

Bacterial Strains	Compound/Control Antibiotics					
	6g		Linezolid		Vancomycin	
	MIC	MBC	MIC	MBC	MIC	MBC
MSSA ATCC 6538	16	> 64	0.5	16	1	2
MSSA NRS 107	16	32	1	16	2	2
MRSA NRS119 (linezolid resistant)	16	32	64	> 64	1	1
MRSA NRS123 (USA400)	32	> 64	1	64	1	1
VRSA 10	16	> 64	0.5	> 64	64	> 64
VRSA 12	32	64	1	32	64	> 64
Methicillin-resistant <i>Staphylococcus epidermidis</i> NRS 101	32	32	0.5	8	2	2
Cephalosporin-resistant <i>Streptococcus pneumonia</i> ATCC 15916	32	32	1	32	1	1
Methicillin-resistant <i>Streptococcus pneumonia</i> ATCC 700677	32	> 64	1	16	2	4
Vancomycin-resistant <i>Enterococcus faecalis</i> ATCC 51299	64	> 64	1	8	32	64
Vancomycin-resistant <i>Enterococcus faecium</i> ATCC 700221	32	32	1	16	> 64	> 64
<i>Listeria monocytogenes</i> ATCC 19111	32	32	0.5	32	1	2

- MSSA: Methicillin-sensitive *Staphylococcus aureus*

- MRSA: Methicillin-resistant *S. aureus*

- VRSA: Vancomycin-resistant *S. aureus*

even more than ciprofloxacin. These results indicate that the bacterial cells have a very good permeability to all the synthetic compounds of our study. This high permeability comes in agreement with the good antimicrobial effect of some of the synthetic compounds because the first step for the antimicrobial agent is to enter the cell and its decrease confer resistance to the cell against the antimicrobial agents¹. While the disagreement between the low antimicrobial activity of most of the compounds and that the cell has a high permeability to them could be caused by one of the resistance mechanisms that could have been developed by the bacterial cell such as the efflux pumps that pump the compound outside the cell after its entry¹. Further studies are needed to determine which mechanisms are involved.

In silico prediction of antibacterial target proteins

The prediction of bacterial target proteins using Schrodinger Maestro 11.9 software showed the interaction between different bacterial proteins and a key ligand (**Figure 1**). Results are shown in **Table 4**. The proteins involved in the of cell wall synthesis including PBP1a, ddlB, and mltB revealed docking score of -3.689, -4.716, and -5.413 kcal/mol; respectively. The DNA-

dependent RNA polymerase beta-subunit protein (*RepC*) used as a target for RNA synthesis inhibition had a docking score of -4.849 kcal/mol. The Isoleucyl- tRNA synthetase (*ileS*) docking score was -4.052 kcal/mol. The target proteins involved in nucleic acid synthesis including DNA gyrase and IV topoisomerase revealed the best docking score (-5.576 and -5.293), respectively. The protein targets of antimetabolites (DHPS and DHFR) exhibited lower binding affinities at -3.573 and -3.950 kcal/mol, respectively. As mentioned above, the best Docking Score is obtained as the most negative value for the active ligands so these results indicate that DNA gyrase and IV topoisomerase have the highest binding activity with the synthetic compounds of our study and could be the target site for their antibacterial action.

Docking and SAR

Based on the above results obtained that the DNA gyrase and IV topoisomerase have the highest binding activity with our synthetic compounds, our next step was to study the interactions of these compounds at the active sites of the topoisomerase II, DNA gyrase, enzyme. Docking was performed with DNA gyrase Chain B crystallographic structure of *S. aureus* that's shown in **Figure 2**.

Table 3. Predicted membrane permeability properties

Ligand	Membrane permeability properties					
	Membrane dG Insert	Membrane HDLD	Membrane GB	Membrane StatePenalty	Log Perm RRCK (cm/s)	Membrane Energy
6k	20.184	19.773	-6.675	0.411	-5.427	1.166
6j	19.062	18.651	-6.410	0.411	-5.324	6.410
6i	19.184	18.773	-6.226	0.411	-5.295	9.184
6h	20.780	20.370	-6.381	0.411	-5.210	-4.145
6g	19.709	19.298	-6.561	0.411	-5.283	5.616
6f	19.002	18.592	-6.420	0.411	-5.276	7.597
6e	19.218	18.808	-6.242	0.411	-5.251	10.442
6d	20.829	20.419	-6.223	0.411	-5.167	-2.645
6c	17.969	17.559	-6.071	0.411	-5.187	12.061
6b	18.260	17.850	-5.846	0.411	-5.165	14.985
6a	20.128	19.717	-6.002	0.411	-5.092	1.615
4k	7.752	7.342	-4.681	0.411	-4.925	27.656
4j	7.970	7.559	-6.659	0.411	-4.878	25.938
4i	7.999	7.588	-6.418	0.411	-4.845	28.948
4h	9.591	9.158	-4.660	0.433	-4.762	20.058
4g	9.210	8.800	-6.471	0.411	-4.863	23.587
4f	8.410	7.999	-6.403	0.411	-4.851	25.393
4e	8.561	8.151	-6.187	0.411	-4.824	28.326
4d	10.474	10.041	-6.343	0.433	-4.754	13.488
4c	7.492	7.081	-5.852	0.411	-4.767	34.495
4b	7.588	7.177	-5.494	0.411	-4.737	37.550
4a	9.448	9.038	-6.291	0.411	-4.663	20.259
Ciprofloxacin	12.935	9.433	-4.437	3.502	-5.296	61.002

The absence of this enzyme in human cells makes it a potent target for many drug discovery methods in treating *S. aureus* infections⁴⁸. The following amino acid residues including Glu50, Asn54, Glu58 and Thr173 present in the ATP-binding pocket of DNA gyrase B is involved in ATPase activity⁴⁹. The results of the *In silico* docking study are shown in (Table 5).

The docking scores of the ligands **6f**, **6j**, **6i**, **6k**, **6d**, and **6e**, **6g**, **6h**, **6b**, **6c** were (-7.425, -7.38, -7.338, -7.321, -7.089, -7.056, -6.977, -6.846, -6.62 and -6.499) kcal/mol, respectively in comparison to -6.176 kcal/mol of ciprofloxacin. Again, the best docking score is the most negative value so we can conclude from these results that those synthetic compounds have the highest binding affinity toward the proposed target site for their

antimicrobial effect, DNA gyrase, an affinity that's even higher than ciprofloxacin. Such results are very good because ciprofloxacin in the first place belongs to the fluoroquinolone class of antibiotics that exert their antibacterial effect through inhibition of the gyrase enzyme¹. The docking scores of the ligands **4k**, **6a**, **4i**, **4h**, **4g**, **4e**, **4d**, **4b**, **4f**, **4j**, and **4a** were (-6.068, -5.806, -5.643, -5.518, -4.962, -4.744, -4.74, -4.388, -3.819, -3.654 and -2.967) kcal/mol, respectively. This result indicates that these compounds have a lower binding affinity with gyrase than ciprofloxacin. Ligand **4k** score value was (-6.068) kcal/mol, approximately equal to the reference ligand value (-6.176 kcal/mol) indicating an almost equal binding affinity to ciprofloxacin towards the gyrase enzyme. Compound **4a** has the lowest binding

Table 4. Docking activity predicted by Schrodinger Maestro 11.9 software

Protein	Name	Target	PDB	Docking score
<i>PBP1a</i>	Penicillin-binding protein 1A		4OON	-3.689
<i>ddlB</i>	D-alanine--D-alanine ligase B	Inhibitors of cell wall synthesis	2DLN	-4.716
<i>mltB</i>	Membrane-bound lytic murein transglycosylase B		1QUT	-5.413
<i>repC</i>	DNA-dependent RNA polymerase beta-subunit	Inhibitors of RNA synthesis	2AUK	-4.849
<i>ileS</i>	Isoleucyl-tRNA synthetase	Inhibitors of protein synthesis	1JZQ	-4.052
<i>TopoIV</i>	IV topoisomerase		3RAE	-5.293
<i>DNA Gyrase</i>	DNA Gyrase	Inhibitors of nucleic acid synthesis	3G75	-5.576
<i>DHPS</i>	Dihydropteroate synthase		1AJ0	-3.573
<i>DHFR</i>	Dihydrofolate Reductase	Antimetabolites	3SRW	-3.950

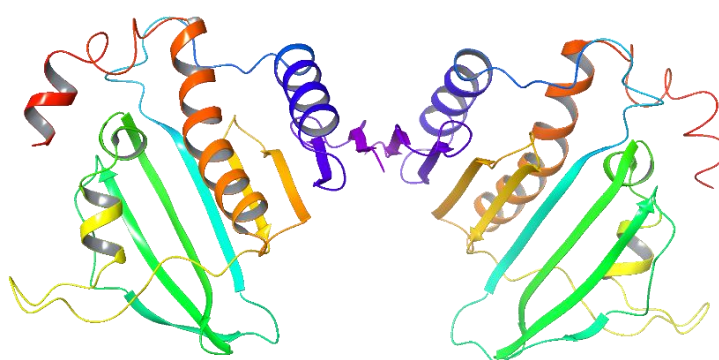


Figure 2. D structure of DNA gyrase of *S. aureus*

affinity to *S. aureus* gyrase enzyme while **6f** has the highest one. Table 6 shows the QSAR of the studied ligands where 3 R groups were presented in the key compound.

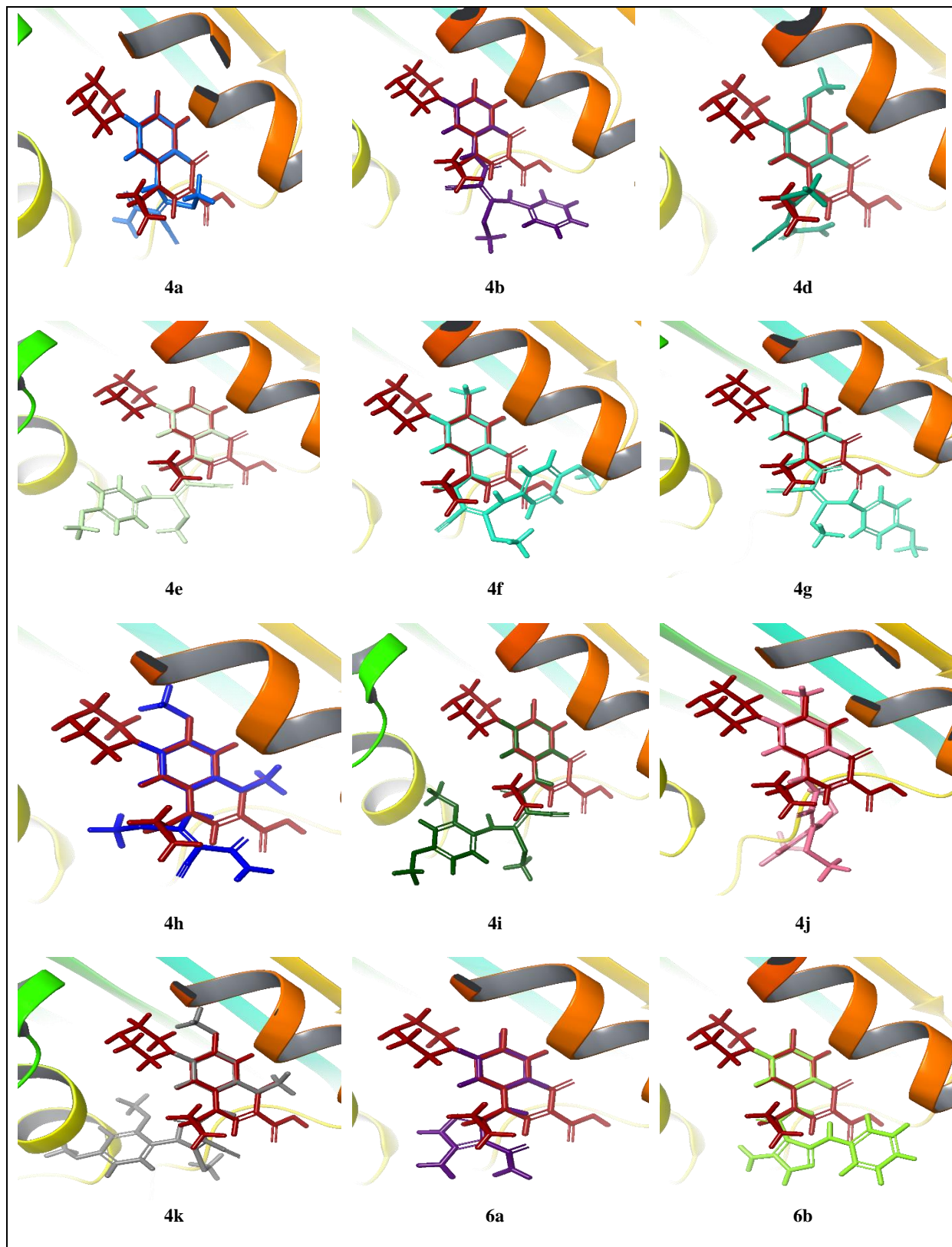
The results shown in the table above confirm the results shown in **Table 5** and indicate a good interaction at the active sites of gyrase enzyme receptors of the same compounds that had good docking score result and a weak reaction of those that had bad scores in **Table 5**. The QSAR results of **6b, 6c, 6d, 6e, 6f, 6i, 6j, 6k** which show a high affinity to bind with the gyrase are contradictory to their high MIC values against MRSA. This can be easily explained by the presence of bacterial resistance mechanism(s) such as efflux pumps which pump the compounds out of the cell, compounds inactivation, changing the target site or any other mechanism¹. On the other hand, the MIC values of the ligand **6g** against MRSA (**Table 1**) showing a good antimicrobial activity are consistent with their *in silico* docking results (**Table 6**) which show a high binding

affinity with DNA gyrase protein. This result strongly suggests that the mode of action of these compounds as antibacterial agents is through affecting the bacterial cell DNA, specifically by inhibiting its DNA gyrase enzyme. Superimposition of ligands was applied to predict the ligand orientation and flexibility in the active site of target protein⁵⁰. The results are shown in **Figure 3**.

These results showed that all the superimposed ligands had the same orientation in the binding pocket of DNA gyrase protein compatible with ciprofloxacin docking position, which means that all the compounds could bind at the same-binding pocket of DNA gyrase. This result confirmed our previous results (**Tables 4, 5 and 6**) which revealed that the target site of our active compounds is the bacterial DNA gyrase enzyme.

Gyrase inhibition assay

Three compounds (**4a, 6i** and **6g**) having different MIC profiles and QSAR values were chosen to detect their DNA gyrase inhibition ability. A set of tubes



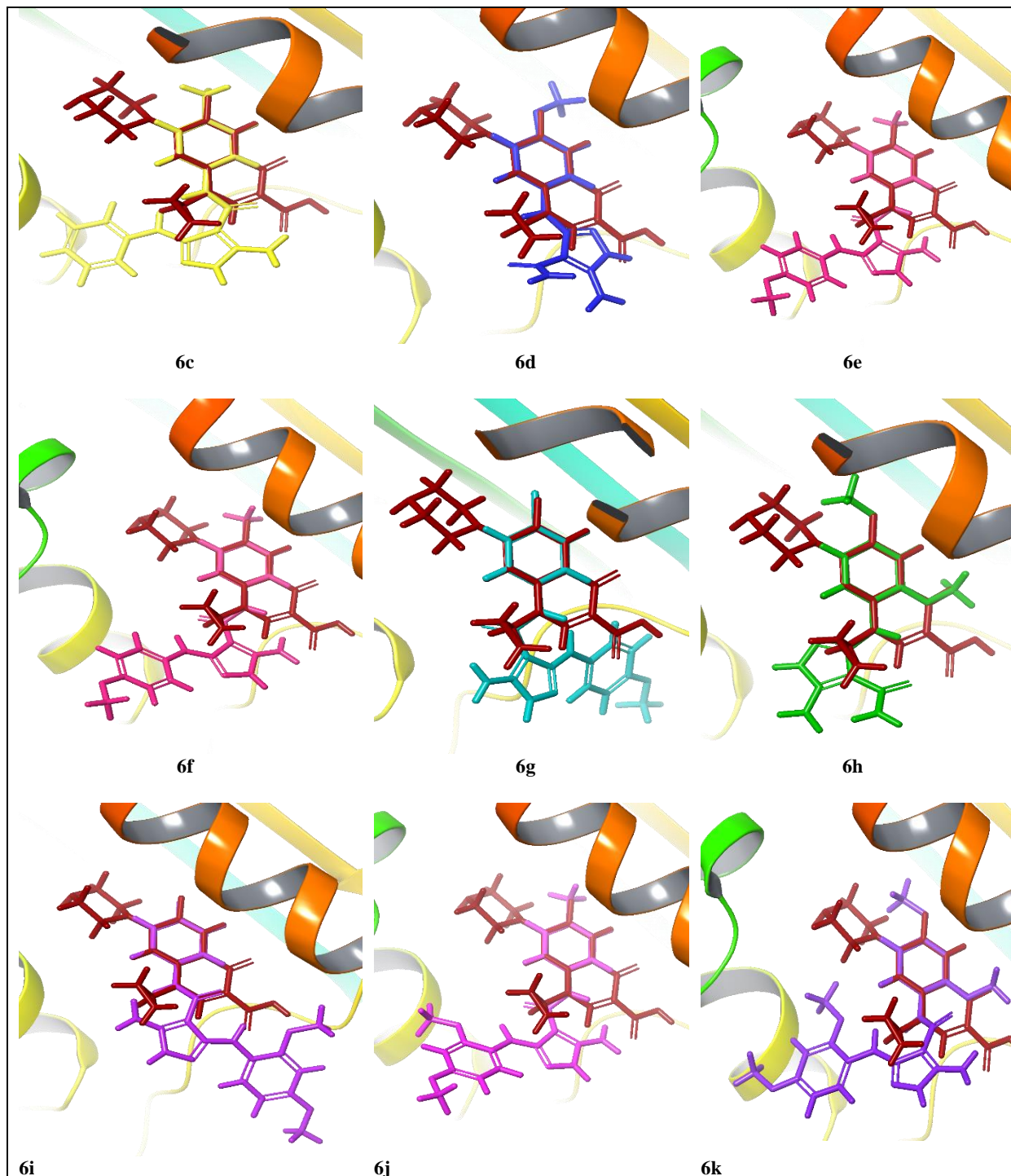


Figure 3. The superimposition of the studied ligands and a reference compound, ciprofloxacin (brown color), with DNA gyrase.

Table 5. *In silico* docking study of ciprofloxacin, and ligands with *S. aureus* DNA gyrase (PDB 3G75)

Ligand	Docking score kcal/mol	Hydrogen bond interactions with Amino Acids	RMS to
6f	-7.425	Asp 81	0.0321
6j	-7.38	Asp 81 and Ser 129	0.0322
6i	-7.338	Asp 81 and Ser 129	0.0278
6k	-7.321	Asn 54, Asp 81 and Ser 55	0.0295
6d	-7.089	Asn 54 and Asp 81	0.0355
6e	-7.056	Asp 81 and Ser 129	0.0238
6g	-6.977	Ser 129	0.0358
6h	-6.846	Ser 129	0.0289
6b	-6.62	Asp 81	0.0320
6c	-6.499	Asp 81	0.0256
4k	-6.068	Ser 129	0.0371
6a	-5.806	Asn 54, Asp 81 and Thr 173	0.0343
4i	-5.643	Ser 129 and Thr 173	0.0306
4h	-5.518	Ser 129 and Thr 173	0.0303
4g	-4.962	Thr 173	0.0285
4e	-4.744	Thr 173	0.0309
4d	-4.74	Asp 81 and Gly 85	0.0296
4b	-4.388	Val 130	0.0288
4f	-3.819	-----	0.0284
4j	-3.654	Val 130	0.0330
4a	-2.967	-----	0.0275
Ciprofloxacin	-6.176	Thr 173	0.0324

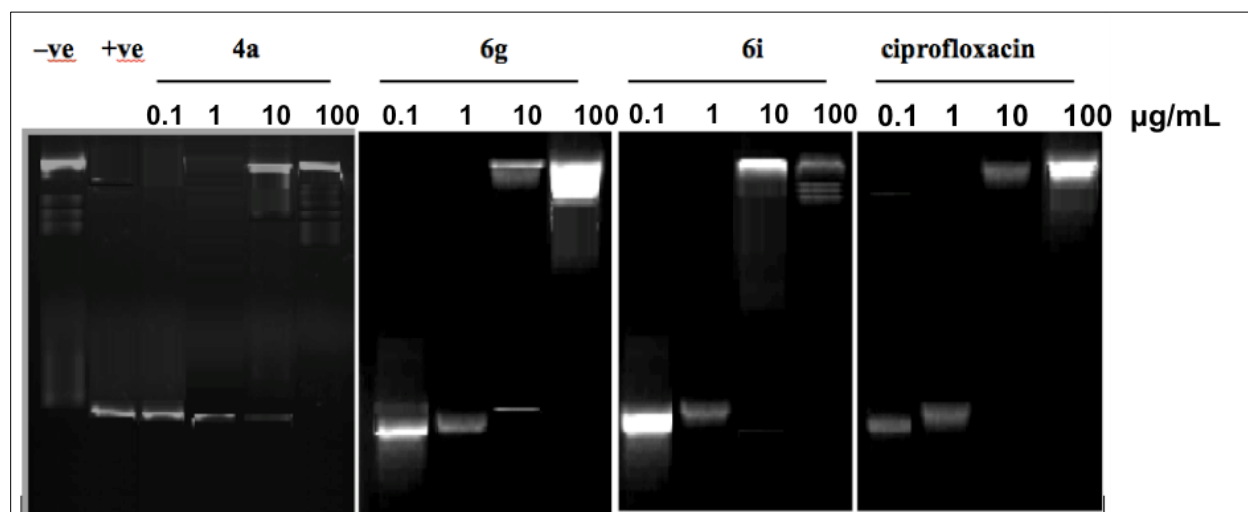
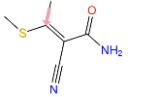


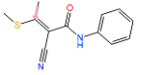





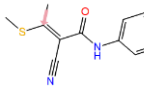
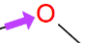

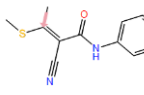


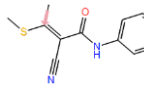


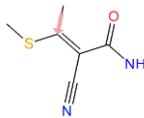


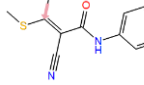

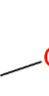
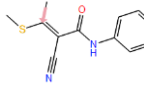

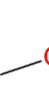
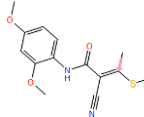


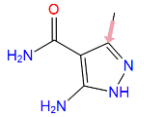


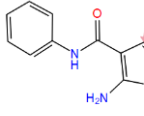


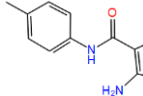


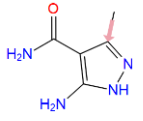
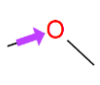

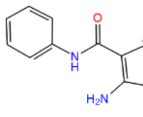
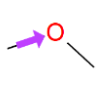

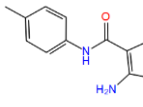
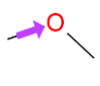

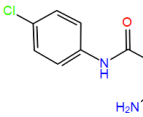
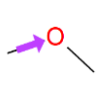

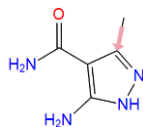


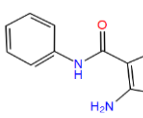


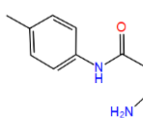
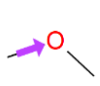

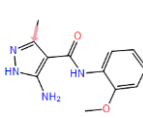
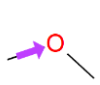



Figure 4. Gel electrophoresis of the supercoiling inhibition experiment with four different concentrations of ciprofloxacin and three synthesized compounds. Negative control is the relaxed plasmid pBR322 without gyrase enzyme or inhibitor, positive control (relaxed plasmid pBR322 with gyrase enzyme and no inhibitor)

Table 6. Quantitative structure–activity relationship (QSAR) of the synthetic compounds

Structure Name	R1	R2	R3	Docking score kcal/mol
4a				-2.967
4b				-4.388
4d				-4.74
4e				-4.744
4f				-3.819
4g				-4.962
4h				-5.518
4i				-5.643
4j				-3.654
4k				-6.068
6a				-5.806
6b				-6.62
6c				-6.499

6d				-7.089
6e				-7.056
6f				-7.425
6g				-6.977
6h				-6.846
6i				-7.338
6j				-7.38
6k				-7.321

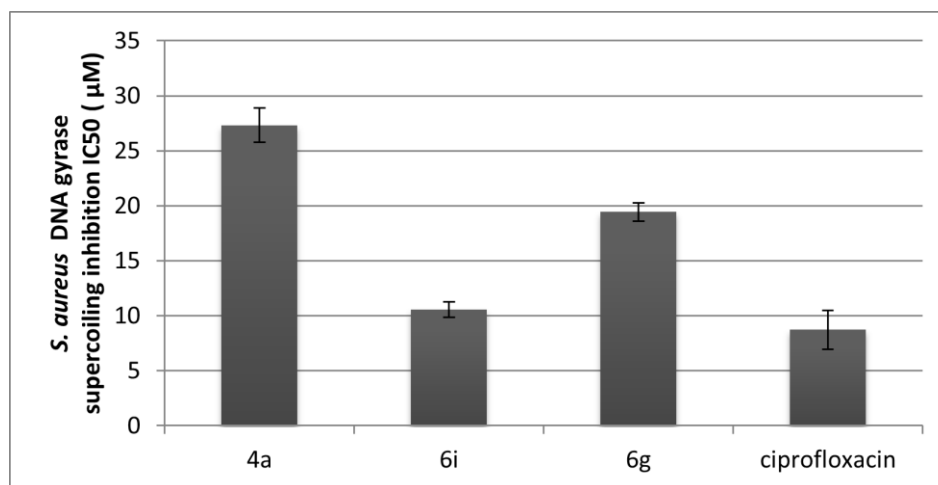


Figure 5. IC₅₀ of the six tested compounds and ciprofloxacin against *S. aureus* DNA gyrase.

was made of a relaxed plasmid pBR322 mixed with the test compound, ciprofloxacin or solvent. The gyrase enzyme was added to all the tubes except the negative control ones. **Figure 4** represents the supercoiled bands photographed by gel documentation system.

The IC₅₀ was assessed for the three tested compounds and ciprofloxacin against *S. aureus* gyrase and the values are represented in **Figure 5**.

The IC₅₀ of compound **4a** was high in comparison to ciprofloxacin, this indicated a low effect on DNA gyrase. This result is consistent with the docking scores of the compound (Tables 5 and 6) where **4a** showed the lowest binding affinity with the gyrase enzyme. The MIC result (**Table 1**) was also consistent with this result as the compound **4a** had a very high value. Together these results mean that **4a** has no antibacterial effect and it does not affect the gyrase enzyme. On the other hand, permeability prediction results (**Table 3**) of **4a** showed that the cell is highly permeable to it. The possible explanation for the collective results of **4a** is that the compound may enter the cell efficiently, but it has no effect on its supposed target site. Compound **6i** showed the highest inhibition of the gyrase enzyme, which was almost equal to the effect of ciprofloxacin. This result is perfectly consistent with both its docking (**Tables 5 and 6**) and permeability results (**Table 3**) as **6i** had almost the highest affinity to gyrase among the tested compounds and a good value in the permeability prediction that's equal to ciprofloxacin, respectively. However, the MIC value of **6i** was so high (**Table 1**) indicating almost no antibacterial effect, this contradiction can be explained by the presence of a resistance mechanism inside the bacterial cell which can inhibit the effect of the compound after it efficiently enters the cell. As for compound **6g**, it showed a very good gyrase inhibitory effect in comparison to ciprofloxacin, this result is again consistent with all our previous findings of **6g**. The compound had the lowest MIC value against MDR *Staphylococcal* strains (**Tables 1 and 2**), a high docking score against DNA gyrase (**Table 5 and 6**) and a good superimposition (**Figure 3**). Compound **6g** also was shown to readily enter the bacterial cell (**Table 3**)

Conclusion

A series of ketene *S,N-acetals* **4a-k** and their pyrazole **6a-k** were synthesized and their structures were established by their spectral data. The results showed significant affinities of binding of some compounds in the docking study. This was confirmed by *in vitro* test with DNA gyrase enzyme presenting this as the possible mode of inhibitory action. The compound **6g** was the most potent compound against some clinically relevant MDR *Staphylococci*. Also the permeability of the bacterial cell to compound **6g** was good and it showed a high docking score against DNA gyrase which was

confirmed by the gyrase inhibition assay in comparison to ciprofloxacin. The collective results of **6g** mean that the compound can efficiently enter the bacterial cell then exerts its action against the DNA gyrase enzyme without being hindered by a resistance mechanism to finally give its bactericidal effect perfectly. Our results present compound **6g** as the most promising candidate as antibacterial agent that could be further modified to enhance its activity against Gram-positive bacteria.

Acknowledgments

The authors would like to thank Dr Mohamed Seleem and Nader Abutaleb for supplying the microbial strains.

Funding

No external funding is included.

Declaration of interest

The authors declare that they have no conflicts of interest regarding the publication of this paper.

CONCLUSION

A series of ketene *S,N-acetals* **4a-k** and their pyrazole **6a-k** were synthesized and their structures were established by their spectral data. The results showed significant affinities of binding of some compounds in the docking study. This was confirmed by *in vitro* test with DNA gyrase enzyme presenting this as the possible mode of inhibitory action. The compound **6g** was the most potent compound against some clinically relevant MDR *Staphylococci*. Also, the permeability of the bacterial cell to compound **6g** was good and it showed a high docking score against DNA gyrase which was confirmed by the gyrase inhibition assay in comparison to ciprofloxacin. The collective results of **6g** mean that the compound can efficiently enter the bacterial cell then exerts its action against the DNA gyrase enzyme without being hindered by a resistance mechanism to finally give its bactericidal effect perfectly. Our results present compound **6g** as the most promising candidate as antibacterial agent that could be further modified to enhance its activity against Gram-positive bacteria.

REFERENCES

1. Munita, J.; Arias, C. Mechanisms of antibiotic resistance. *Microbiol. Spectr.* **2016**, <https://doi.org/10.1128/microbiolspec.VMBF-0016-2015>
2. Lakhundi, S.; Zhang, K. Methicillin-Resistant staphylococcus aureus: molecular characterization, evolution, and epidemiology. *Clin. Microbiol. Rev.* **2018**, *31* (4), e00020-18. <https://doi.org/10.1128/CMR.00020-18>

- Chitra SR, Ramalakshmi N, Arunkumar S, Manimegalai P. A comprehensive review on DNA gyrase inhibitors. *Infect. Disord. Drug Targets* **2020**, 20 (6), 765-777. doi:10.2174/1871526520666200102110235
- Kathiravan, M. K.; Khilare, M. M.; Nikoومانesh, K.; Chothe, A. S.; Jain, K. S. Topoisomerase as target for antibacterial and anticancer drug discovery. *J. Enzyme Inhib. Med. Chem.* **2013**, 28 (3), 419-435. <https://doi.org/10.3109/14756366.2012.658785>
- Mazurek, Ł.; Ghilarov, D.; Michalczyk, E.; Pakosz, Z.; Metelev, M.; Czystoczóń, W.; Wawro, K.; Behroz, I.; Dubiley, S.; Süßmuth, R. D.; Heddle, J. G. Pentapeptide repeat protein QnrB1 requires ATP hydrolysis to rejuvenate poisoned gyrase complexes, *Nucleic Acids Res.* **2021**, 49 (3), 1581-1596. <https://doi.org/10.1093/nar/gkaa1266>
- Wise, R.; Piddock, L. The need for new antibiotics. *The Lancet.* **2010**, [https://doi.org/10.1016/S0140-6736\(10\)60266-8](https://doi.org/10.1016/S0140-6736(10)60266-8)
- Xu, L.; Xu, Z.; Zhang, G.; Zhou, K.; Zhai, Z. Synthesis, characterization and biological activities of novel acrylamide compounds. *Chem. Res. Chin. Univ.* **2008**, 24 (5), 575-578. [https://doi.org/10.1016/S1005-9040\(08\)60121-X](https://doi.org/10.1016/S1005-9040(08)60121-X)
- Elgiushy, H.; Hammad, S.; Hassan, A. S.; Aboutaleb, N.; Abouzid, K. Acrylamide moiety, a valuable fragment in medicinal chemistry: insight into synthetic methodologies, chemical reactivity and spectrum of biological activities of acrylamide derivatives. *J. Adv. Pharm. Res.* **2018**, 2 (4), 221-237. <https://doi.org/10.21608/aprh.2018.2839.1049>
- Avalos-Alanís, F. G.; Hernández-Fernández, E.; Carranza-Rosales, P.; López-Cortina, S.; Hernández-Fernández, J.; Ordóñez, M.; Guzmán-Delgado, E. N.; Morales-Vargas, A.; Velázquez-Moreno, V. M.; Santiago-Mauricio, M. G. Synthesis, antimycobacterial and cytotoxic activity of α,β -unsaturated amides and 2,4-disubstituted oxazoline derivatives. *Bioorganic Med. Chem. Lett.* **2017**, 27 (4), 821-825. <https://doi.org/10.1016/j.bmcl.2017.01.024>
- Kalaria, P. N.; Satasia, P. S.; Raval, D. K. Synthesis, characterization and pharmacological screening of some novel 5-imidazopyrazole incorporated polyhydroquinoline derivatives. *Eur. J. Med. Chem.* **2014**, 78, 207-216. <https://doi.org/10.1016/j.ejmech.2014.02.015>
- Mizuhara, T.; Kato, T.; Hirai, A.; Kurihara, H.; Shimada, Y.; Taniguchi, M.; Maeta, H.; Togami, H.; Shimura, K.; Matsuoka, M.; Okazaki, S.; Takeuchi, T.; Ohno, H.; Oishi, S.; Fujii, N. Structure-activity relationship study of phenylpyrazole derivatives as a novel class of anti-HIV agents. *Bioorganic Med. Chem. Lett.* **2013**, 23 (16) 4557-4561. <https://doi.org/10.1016/j.bmcl.2013.06.026>
- Rostom, S. A.; Shalaby, M. A.; El-Demellawy, M. A. Polysubstituted Pyrazoles, Part 5. Synthesis of new 1-(4-chlorophenyl)-4-hydroxy-1H-pyrazole-3-carboxylic acid hydrazide analogs and some derived ring systems. A novel class of potential antitumor and anti-HCV agents. *Eur. J. Med. Chem.* **2003**, 38 (11-12), 959-974. <https://doi.org/10.1016/j.ejmech.2003.08.003>
- Shih, S. R.; Chu, T.; Reddy, G.; Tseng, S.; Chen, H.; Tang, W.; Wu, M.-S.; Yeh, J.-Y.; Chao, Y.-S.; Hsu, J. T. A.; Hsieh, H.-P.; Horng, J.-T. Pyrazole compound BPR1P0034 with potent and selective anti-influenza virus activity. *J. Biomed Sci.* **2010**. <https://doi.org/10.1186/1423-0127-17-13>
- Gaikwad, N. D.; Patil, S.; Bobade, V. Synthesis and antimicrobial activity of novel thiazole substituted pyrazole derivatives. *J. Heterocyclic Chem.*, **2013**, 50 (3), 519-527. <https://doi.org/10.1002/jhet.1513>
- Hafez, H. N.; Alshammari, A.; El-Gazzar, A. Facile heterocyclic synthesis and antimicrobial activity of polysubstituted and condensed pyrazolopyranopyrimidine and pyrazolopyranotriazine derivatives. *Acta Pharmaceutica* **2015**, 65, 399-412. <https://doi.org/10.1515/acph-2015-0037>
- Hafez, H. N.; El-Gazzar, A.; Al-Hussain, S. Novel pyrazole derivatives with oxa/thiadiazolyl, pyrazolyl moieties and pyrazolo[4,3-d]pyrimidine derivatives as potential antimicrobial and anticancer agents. *Bioorganic Med. Chem. Lett.* **2016**, 26 (10), 2428-2433. <https://doi.org/10.1016/j.bmcl.2016.03.117>
- Refat, H. M.; Fadda, A. A. Synthesis and antimicrobial activity of some novel hydrazide, pyrazole, triazine, isoxazole, and pyrimidine derivatives. *J. Heterocyclic Chem.*, **2016**, 53 (4), 1129-1137. <https://doi.org/10.1002/jhet.2369>
- Ahn, M.; Gunasekaran, P.; Rajasekaran, G.; Kim, E. Y.; Lee, S.-J.; Bang, G.; Cho, K.; Hyun, J.-K.; Lee, H.-J.; Jeon, Y. H.; Kim, N.-H.; Ryu, E. K.; Shin, S. Y.; Bang, J. K. Pyrazole derived ultra-short antimicrobial peptidomimetics with potent anti-biofilm activity. *Eur. J. Med. Chem.* **2017**, 125, 551-564. <https://doi.org/10.1016/j.ejmech.2016.09.071>
- Abd El-All, A. S.; Hassan, A. S.; Osman, S. A.; Yosef, H. A. A.; Abdel-Hady, W. H.; El-Hashash, M. A.; Atta-Allah, S. R.; Ali, M. M.; El Rashedy, A. A. Synthesis, characterization and biological evaluation of new fused triazine derivatives based on 6-methyl-3-thioxo-1,2,4-triazin-5-one. *Acta Pol. Pharm.*, **2016**, 73 (1), 79-92.
- El-Naggar, M.; Hassan, A. S.; Awad, H. M.; Mady,

- M. F. Design, synthesis and antitumor evaluation of novel pyrazolopyrimidines and pyrazoloquinazolines. *Molecules*, **2018**, *23* (6), 1249 <https://doi.org/10.3390/molecules23061249>
21. Osman, S. A.; Mousa, H. A.; Yosef, H. A. A.; Hafez, T. S.; El-Sawy, A. A.; Abdallah, M. M.; Hassan, A. S. Synthesis, characterization and cytotoxicity of mixed ligand Mn(II), Co(II) and Ni(II) complexes. *J. Serb. Chem. Soc.* **2014**, *79* (8), 953-964. <https://doi.org/10.2298/JSC130813134O>
22. Mukhtar, S. S.; Hassan, A. S.; Morsy, N. M.; Hafez, T. S.; Saleh, F. M.; Hassaneen, H. M. Design, synthesis, molecular predication and biological evaluation of pyrazole-azomethine conjugates as antimicrobial agents. *Synth. Commun.*, **2021**, *51* (10), 1564-1580. <https://doi.org/10.1080/00397911.2021.1894338>
23. Abdelghany, A. M.; Khatib, T. K.; Hassan, A. S. Copper-based glass-ceramic as an efficient catalyst in the synthesis of pyrazolo[1,5-*a*]pyrimidine under solvent-free condition with docking validation as COVID-19 main protease (Mpro) inhibitor. *Bull. Chem. Soc. Ethiop.*, **2021**, *35* (1), 185-196. <https://dx.doi.org/10.4314/bcse.v35i1.16>
24. Hassan, A. S.; Awad, H. M.; Magd-El-Din, A. A.; Hafez, T. S. Synthesis and *in vitro* antitumor evaluation of novel Schiff bases. *Med. Chem. Res.*, **2018**, *27* (3), 915-927. <https://doi.org/10.1007/s00044-017-2113-5>
25. Hassan, A. S.; Hafez, T. S. Antimicrobial activities of ferrocenyl complexes: A review. *J. App. Pharm. Sci.*, **2018**, *8* (5), 156-165. <https://doi.org/10.7324/JAPS.2018.8522>
26. Hassan, A.S. Mixed isatin with 3-(2-(aryl)hydrazono)acetylacetone Mn(II), Co(II) and Ni(II) complexes: antibacterial evaluation and molecular properties prediction. *Bull. Chem. Soc. Ethiop.*, **2020**, *34* (3), 533-541. <https://dx.doi.org/10.4314/bcse.v34i3.9>
27. Hassan, A. S.; Askar, A. A.; Naglah, A. M.; Almehezia, A. A.; Ragab, A. Discovery of new Schiff bases tethered pyrazole moiety: Design, synthesis, biological evaluation, and molecular docking study as dual targeting DHFR/DNA gyrase inhibitors with immunomodulatory activity. *Molecules* **2020**, *25* (11), 2593. <https://doi.org/10.3390/molecules25112593>
28. Hassan, A. S.; Askar, A. A.; Nossier, E. S.; Naglah, A. M.; Moustafa, G. O.; Al -Omar, M. A. Antibacterial evaluation, *in silico* characters and molecular docking of Schiff bases derived from 5-aminopyrazoles. *Molecules*, **2019**, *24* (17), 3130. <https://doi.org/10.3390/molecules24173130>
29. Fadda, A. A.; Bondock, S.; Etman, R. H. A. cyanoacetamide derivatives as synthons in heterocyclic synthesis. *Turk J Chem.*, **2008**, *32*, 259-286.
30. Hafez, T. S.; Osman, S. A.; Yosef, H. A. A.; Abd El-All, A. S.; Hassan, A. S.; El-Sawy, A. A.; Abdallah, M. M.; Youns, M. Synthesis, structural elucidation and *in vitro* antitumor activities of some pyrazolopyrimidines and Schiff bases derived from 5-amino-3-(arylamino)-1*H*-pyrazole-4-carboxamides. *Sci. Pharm.*, **2013**, *81* (2), 339-357. <http://dx.doi.org/10.3797/scipharm.1211-07>
31. Hassan, A. S.; Moustafa, G. O.; Awad, H. M.; Nossier, E. S.; Mady. M. F. Design, synthesis, anticancer evaluation, enzymatic assays, and a molecular modeling study of novel pyrazole-indole hybrids. *ACS Omega*, **2021**, *6* (18), 12361-12374. <https://doi.org/10.1021/acsomega.1c01604>
32. Hassan, A. S.; Masoud, D. M.; Sroor, F. M.; Askar, A. A. Synthesis and biological evaluation of pyrazolo[1,5-*a*]pyrimidine-3-carboxamide as antimicrobial agents. *Med. Chem. Res.*, **2017**, *26* (11), 2909-2919. <https://doi.org/10.1007/s00044-017-1990-y>
33. Hassan, A. S.; Hafez, T. S.; Osman, S. A. Synthesis, characterization, and cytotoxicity of some new 5-aminopyrazole and pyrazolo[1,5-*a*]pyrimidine derivatives. *Sci. Pharm.*, **2015**, *83* (1), 27-39. <http://dx.doi.org/10.3797/scipharm.1409-14>
34. Clinical And Laboratory Standards Institute, *Performance Standards for Antimicrobial Susceptibility Testing*, Informational Supplement, M100-S, CLSI, Wayne, Pa, USA, 26th edition, **2016**.
35. Leung, S. S. F.; Mijalkovic, J.; Borrelli, K.; Jacobson, M. P. Testing physical models of passive membrane permeation. *J. Chem. Inf. Model.* **2012**, *52* (6), 1621-1636. <https://doi.org/10.1021/ci200583t>
36. Rezai, T.; Yu, B.; Millhauser G. L.; Jacobson, M. P.; Lokey, R. S. Testing the conformational hypothesis of passive membrane permeability using synthetic cyclic peptide diastereomers. *J. Am. Chem. Soc.* **2006**, *128* (8), 2510-2511. <https://doi.org/10.1021/ja0563455>
37. Schrödinger Release (2019)-1, 'Prime', New York, USA, **2019**.
38. Jorgensen, W. L.; Maxwell, D. S.; Tirado-Rives, J. Development and testing of the opls all-atom force field on conformational energetics and properties of organic Liquids. *J. Am. Chem. Soc.* **1996**, *118* (45), 11225-11236. <https://doi.org/10.1021/ja9621760>
39. Kaminski, G. A.; Friesner, R. A.; Tirado-Rives, J.; Jorgensen, W. L. Evaluation and reparametrization of the OPLS-AA force field for proteins *via* comparison with accurate quantum chemical calculations on peptides. *J. Phys. Chem. B* **2001**,

- 105 (28), 6474-6487. <https://doi.org/10.1021/jp003919d>
40. Schrodinger, L. *MacroModel, Version 10.2*. New York (NY), **2013**.
41. Ronkin, S. M.; Badia, M.; Bellon, S.; Grillot, A.-L.; Gross, C. H.; Grossman, T. H.; Mani, N.; Parsons, J. D.; Stamos, D.; Trudeau, M.; Wei, Y.; Charifson, P. S. Discovery of Pyrazolthiazoles as Novel and Potent Inhibitors of Bacterial Gyrase. *Bioorganic Med. Chem. Lett.* **2010**, *20* (9), 2828-2831. <https://doi.org/10.1016/j.bmcl.2010.03.052>
42. Friesner, R. F.; Murphy, R. B.; Repasky, M. P.; Frye, L. L.; Greenwood, J. R.; Halgren, T. A.; P. C.; Sanschagrin, Mainz, D. T. Extra precision glide: docking and scoring incorporating a model of hydrophobic enclosure for protein-ligand complexes. *J. Med. Chem.* **2006**, *49* (21), 6177-6196. <https://doi.org/10.1021/jm051256o>
43. Naseem, S.; Khalid, M.; Tahir, M. N.; Halim, M. A.; Braga, A. C. A.; Naseer, M. M.; Shafiq, Z. Synthesis, structural, DFT studies, docking and antibacterial activity of a xanthene based hydrazone ligand. *J. Mol. Struct.* **2017**, *1143*, 235-244. <https://doi.org/10.1016/j.molstruc.2017.04.093>
44. Bondock, S.; Nasr, T.; Zaghary, W.; Chantrapomma, S.; Ghabbour, H.; Fun, H.-K. Novel diastereoselective synthesis and x-ray crystallographic studies of new (*E*)-2-cyano-N-(4-ethoxyphenyl)-3-methylthio-3-(substituted-amino)acrylamides. *Mol. Cryst. Liq. Cryst.* **2014**, *605*, 165-178. <https://doi.org/10.1080/15421406.2014.885354>
45. Khatab, T. K.; Hassan, A. S.; Hafez, T. S. V₂O₅/SiO₂ as an efficient catalyst in the synthesis of 5-aminopyrazole derivatives under solvent free condition. *Bull. Chem. Soc. Ethiop.*, **2019**, *33* (1), 135-142. <https://dx.doi.org/10.4314/bcse.v33i1.13>
46. Al-Adiwish, W. M.; Tahir M. I. M.; Adnalizawati, A.; Hashim, S. F.; Ibrahim, N.; Yaacob, W. A. Synthesis, antibacterial activity and cytotoxicity of new fused pyrazolo[1,5-a]pyrimidine and pyrazolo[5,1-c][1,2,4]triazine derivatives from new 5-aminopyrazoles. *Eur. J. Med. Chem.* **2013**, *64*, 464-476. <https://doi.org/10.1016/j.ejmech.2013.04.029>
47. Leung, S. S. F.; Mijalkovic, J.; Borrelli, K.; Jacobson, M. P. <https://pubs.acs.org/action/doSearch?field1=Contrib&text1=Kenneth++BorrelliTesting> physical models of passive membrane permeation. *J. Chem. Inf. Model.* **2012**, *52* (6), 1621-1636 <https://doi.org/10.1021/ci200583t>
48. Leung, S. S. F.; Sindhikara, D.; Jacobson, M. P. Simple predictive models of passive membrane permeability incorporating size-dependent membrane-water partition. *J. Chem. Inf. Model.* **2016**, *56* (5), 924-929. <https://doi.org/10.1021/acs.jcim.6b00005>
49. Jagadeesan, G.; Vijayakuma, V.; Palayam, M.; Suresh, G.; Krishnaswamy, G.; Aravindhan, S.; Peters, G. H. Pyrazole based inhibitors against enzymes of *Staphylococcus aureus*: a computational study. *J. Proteomics. Bioinform.* **2015**, *8* (7), 142-148. <https://doi.org/10.4172/jpb.1000362>
50. Roychowdury, D.; Talukdar, P.; Talapatra, S. N. Established leaf flavonoids as phytoligands from andrographis *Andrographis paniculata* (Burm. f.) Wall. Ex Nees for antibacterial activity against bacterial DNA-gyrase B receptor: an *in silico* approach. *World J. Adv. Healthc. R.* **2020**, *4* (5), 78-84.
51. Stockmann, H.; Bronowska, A.; Syme, N. A.; Thompson, G. S.; Kalverda, A. P.; Warriner, S. L.; Homans, S. W. residual ligand entropy in the binding of *p*-substituted benzenesulfonamide ligands to bovine carbonic anhydrase II. *J. Am. Chem. Soc.* **2008**, *130* (37), 12420-12426. <https://doi.org/10.1021/ja803755m>